RSC Advances

ROYAL SOCIETY OF CHEMISTRY

www.rsc.org/advances

MFA Zeotype Catalyst: A Greener Approach for The Synthesis of INH Azomethine Scaffolds

Devendra S. Raghuvanshi,[a] Pramod P. Mahulikar,[a] Jyotsna S. Meshram*[a]

[a]School of Chemical Sciences, North Maharashtra University, Jalgaon (MS) India.

drjsmeshram@gmail.com

Herein, we are reporting the green and efficient synthesis of some pharmacologically important azomethine derivatives of INH using Modified Fly Ash (MFA) as an excellent zeotic solid acid catalyst. The catalyst by the virtue of its terminal hydroxyl groups, forms a hydrogen bonding with the carbonyl compounds which activates the reactants for condensation. The MFA is confined for various aspects like crystallanity, porosity, elemental composition, linkages and also for its stability which is confirmed with the help of some physical spectral analysis like XRD, BET, EDS, FTIR and TGA analysis. The effective MFA synthesis is achieved by the calcination of aqueous mixture of fly ash with ferric chloride successfully incorporating the iron to generate slightly acidic crystalline zeotic material which served an energy efficient catalyst by accessing the reaction at room temperature.

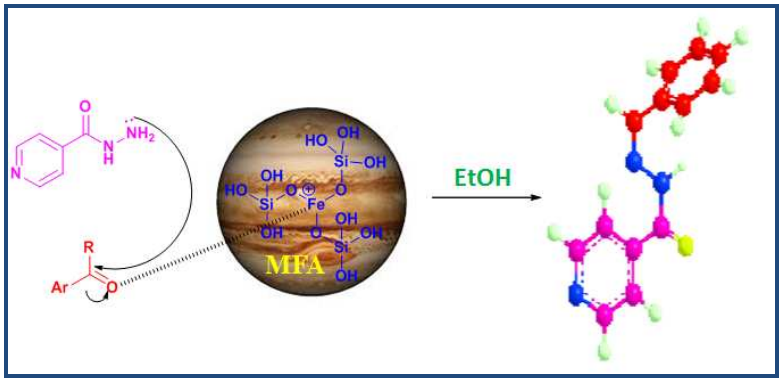

Keywords: MFA, Zeolite, Energy efficiency, Solid support, Green synthesis

Introduction

Now a days, owing to environmental restrictions on emissions covered in several legislations throughout the world, non-polluting and atom-efficient catalytic technologies are attracting much attention.[1] The use of acid catalysts is very common in the chemical and refinery industries,[2] and the technologies employing highly corrosive, hazardous and polluting liquid acids are being replaced with solid acids,[3] for instance, acid treated clays, zeolites,[4] zeotypes,[5] ion-exchange resins[6] and metal oxides.[7]

Fly ash is the solid waste residue produced from coal, oil and biomass combustion comprises the fine particles that are rise above with flue gases.[8] It is estimated that efficient disposal of fly ash is a worldwide issue because of the huge amount produced and its harmful effects on the environment.[9] Now a days, the synthesis of zeolites with the use of fly ash is attracting lots of attention due to its peculiar properties in catalysing many reactions.[10] Fly ash acts as a rich source of silica in the synthesis of zeolite which easily recombines with

transition metals on hydrothermal or calcination treatment forming highly branched zeotype geometry of molecule.[11]

Isonicotinic acid hydrazide or Isonicotinylhydrazide, commonly known as isoniazide (INH),[12] is an bacteriostatic/bactericidal agent used to treat infections caused by *Mycobacterial tuberculosis*.[13] It is a first line tubercular prodrug activated on the surface of *M. tuberculosis* by katG enzyme to isonicotinic acid and is active against susceptible bacteria only during bacterial cell division.[14] INH can form Schiff's bases with carbonyl compounds and their metal chelate exhibits anticancer activity.[15] The azomethine derivatives of INH derived by the condensation with 3,4-dimethoxy benzaldehyde and 3,4,5-trimethoxy benzaldehyde are known to show antimicrobial activity[16] while those derived by 3-methoxy-4-hydroxy benzaldehyde and 4-oxypropane benzaldehyde are known as most potent antioxidents with significant hydrogen peroxide scavenging agents.[6]

The present study throws light on the development of newer catalyst by the modification of fly ash, the waste generated in thermal power plant. The catalyst is found as a highly energy efficient in the synthesis of azomethine derivatives of INH. The reports up to now have utilized acetic acid,[17] hydrochloric acid as catalyst on reflux and also some reports are without catalyst but on reflux at least for 2-3 hours.[18] Hence looking into its wide scope, development of new molecular entities with the special reference to azomethines INH with the MFA at RT is reported in present study.

Experimental

Materials

All the materials (like ferric chloride, urea, INH and aryl carbonyl compounds) are purchased from SD Fine Chemicals Pvt. Ltd, Mumbai (India). The fly ash is collected from the nearby area of the thermal power plant, Deep Nagar, Tal- Bhusawal, Dist – Jalgaon – 425 001 (MS), India. The fly ash is sampled in equal volumes from four directions of plant and mixed thoroughly to make homogeneous mass.

Methods

Synthesis of MFA Zeotype Catalyst

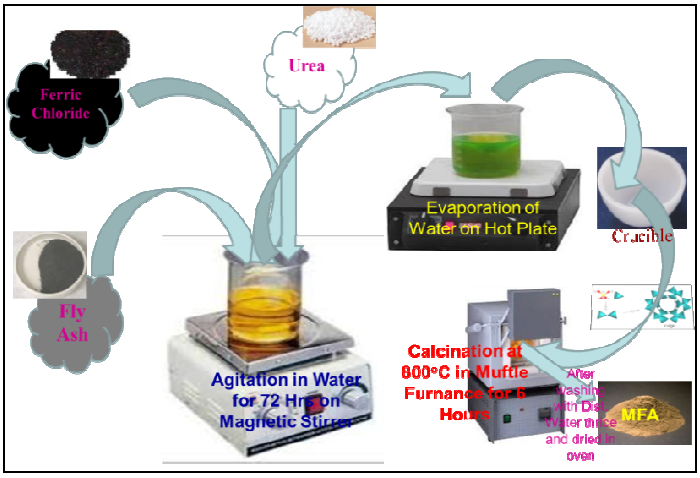

Fig. 1 Schematic Diagram of MFA Synthesis

5 g fly ash, 1 g ferric chloride and 1 g urea are agitated in water for 72 hours to obtain the homogeneous mixture and then the water is evaporated on hot plate to obtain semi-solid material. The fly ash is loaded with ferric chloride and urea is then charged in quartz crucible and subjected for calcination in muffle furnace at 800^{o}C for 6 hours. Ferrous reacts with silicates present in fly ash to forms ferrous silicates and the channels/pores are created due to decomposition of urea at this elevated temperature. The obtained mesoporous material is then properly stirred in distilled water (3 X 100 ml) to remove unreacted ferric chloride and urea. The wet solid is dried and activated at 200^{o}C for 12 hours in oven to form the MFA.

Reaction Scheme

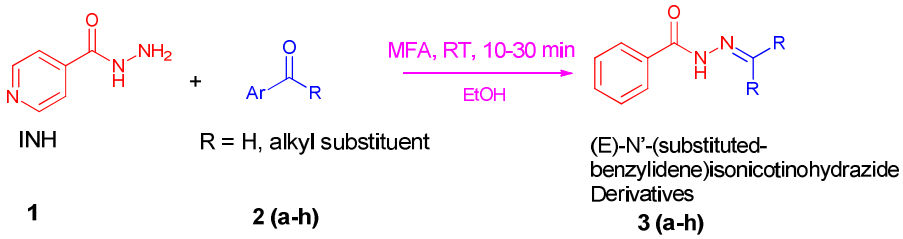

Scheme 1. Synthesis of (E)-N'-(Substituted-benzylidene) isonicotinohydrazide Derivatives

INH (10 mmol), aromatic aldehydes or ketones (10 mmol) (2a-h) and catalytic amount of MFA (10% w/w of reaction mass) are taken in EtOH and mixed thoroughly. The condensation reaction at RT yields N-(substituted benzylidene) isonicotinohydrazide derivatives in 10-30 min (3a-h). In the synthesis, firstly measured quantity of INH is taken in round bottom flask, followed by addition of measured quantity of aldehydes or ketones. Then the mixture is mixed thoroughly on stirring and addition of MFA is executed. The reaction is continuously observed on TLC technique for the formation of product. After that reaction mass is filtered through whatmann filter paper and washed with water. The obtained product then recrystallized with pure ethanol separates the MFA as residue on filter paper and pure product reappears in filtrate on cooling.

Proposed Mechanism:

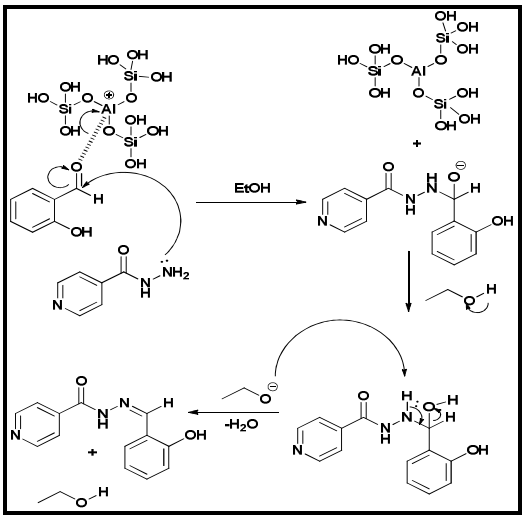

The mechanism proposed reveals the catalytic role of MFA in the synthesis of azomethine derivatives of INH. The core functional group responsible for its catalytic behaviour is ferrous silicates having the Fe-O-Si linkages present on the surface and in the pore voids of MFA which polarizes the aldehydes or ketones and increases the electron deficiency at carbonyl carbon centre. The lone pair of amine nitrogen present in INH easily attacks on sufficiently electron deficient carbonyl carbon followed by abstraction of acidic proton from solvent and further dehydration leads to formation of azomethine derivatives of INH.

Optimization of Efficient Amount of MFA Required for Excellent Yield (3a)

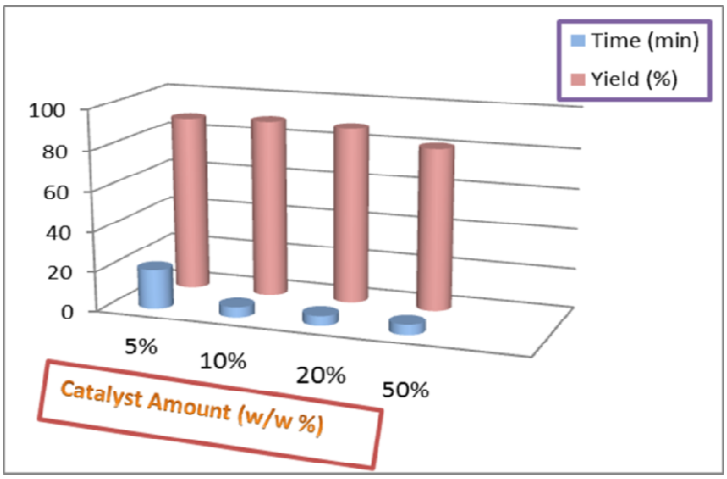

Chart 1

The reaction is tested for different amount of catalyst to optimise the proper amount of catalyst for the best results in terms of time and yield in the synthesis of *(E)-N'*-benzylideneisonicotinohydrazide (3a). The study (Chart 1) depicts the low amount of catalyst leads for long reaction time while high amounts results in the decrease in yields of reaction. The optimistic amount is found to be 10% w/w of reaction mass.

Catalyst Reusability Study (3a)

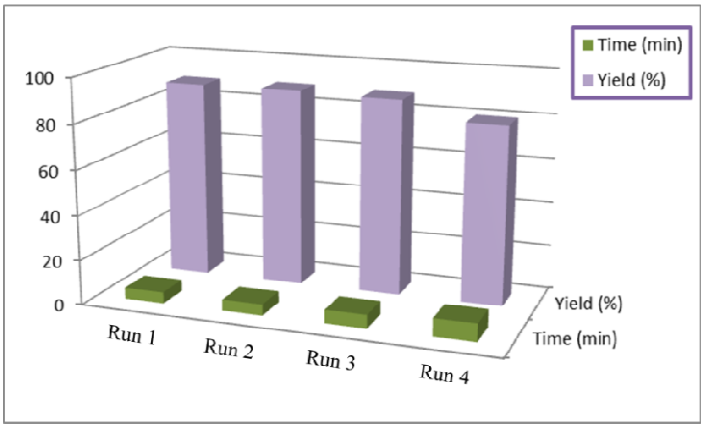

Chart 2

The catalyst is subjected to study its reusability in the synthesis of *(E)-N'*-benzylideneisonicotinohydrazide (3a) (Chart 2). The MFA recovered on filtration from previous step is firstly wash with hot EtOH and water. Thus, purified MFA is subjected for activation at 120^{o}C in oven for 4 hours. The activated MFA is subjected for its catalytic efficiency again in next set of reaction. The study reveals that the MFA can be used efficiently up to 3 times after its recovery from previous synthesis.

Results and Discussions

Characterization of MFA

IR Analysis

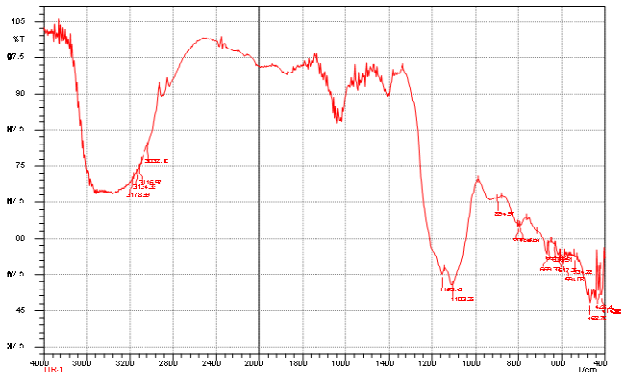

Fig. 2 FTIR of MFA

The MFA having terminal –OH group estimated by IR spectra (Fig. 2) has peaks at 3500 cm^{-1} to 3300 cm^{-1}. The peak at 1153 cm^{-1} and 1103 cm^{-1} are attributed to Si-O linkages while the peak at 894 cm^{-1} is a evidence of the presence of Fe-O bond. The bonds at 800 cm^{-1}, 790 cm^{-1} and 594 cm^{-1} shows the presence of Fe-O-Si linkages.

XRD Analysis

As already been concluded from IR analysis (Fig. 2) and EDXS analysis the incorporation of iron metal as iron silicate executed successfully, no modification in XRD pattern (Fig. 3) is the evident by the replacement of aluminium or other trace impurities with iron conserving the geometry of crystal lattice. X ray difractogram is done on a Brucker D8 advanced instrument with Cu-Kα radiation (λ=0.514nm). The X ray diffraction pattern is recorded over 0 to 80^{o} (2θ degree).

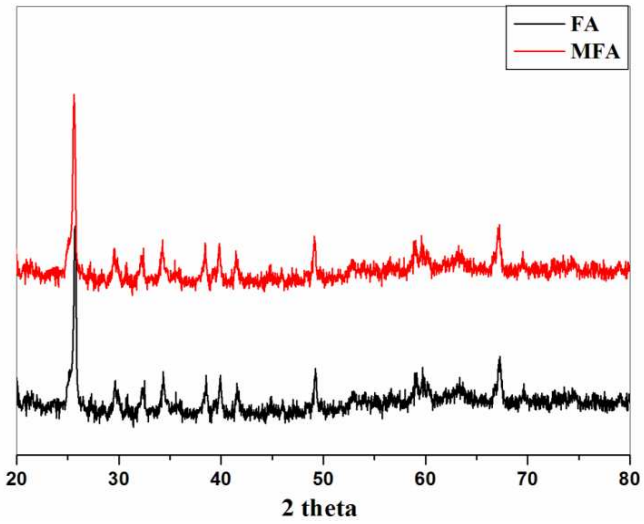

Fig. 3 Powder XRD Analysis

FESEM Analysis

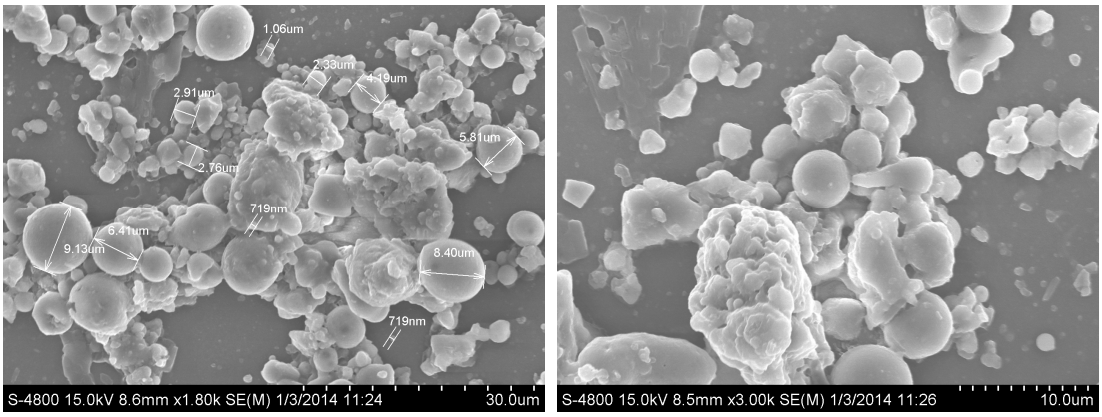

Fig. 4 & 5 FESEM Images of MFA

FESEM images (Fig. 4 & 5) are taken on Hitachi S4800 instrument after gold plating applied with the help of Hitachi Ion Sputter E1010 instrument. The FESEM analysis shows the MFA has an spherical geometry. The particles having the diameter in range of 1 μm to 10 μm which is in accordance to the spherical dimension.

EDXS Analysis

The EDXS spectra recorded on Brucker X Flash Detector shows the suceessful incorporation of iron in fly ash collected from thermal power plnt to form mesoporous ferrous silicates. The composition contains 8% iron and 17% aluminium while silica and oxygen present in 25% and 50% respectively.

BET Analysis

The BET surface area analysis (Fig. 6 & 7) generated the loop like graph upon nitrogen absorption and desorption technique. The loop is the evidence for the porosity of the MFA. When pressured N_2 is applied, it absorbs nitrogen readily and as soon as pressure is released, it releases the nitrogen slowly as the nitrogen is get entrapped in the pores of catalyst. The pore size distribution curve (Fig. 8) shows that the catalyst pore radii size is 6 nm belonging to the class of mesoporous compounds.

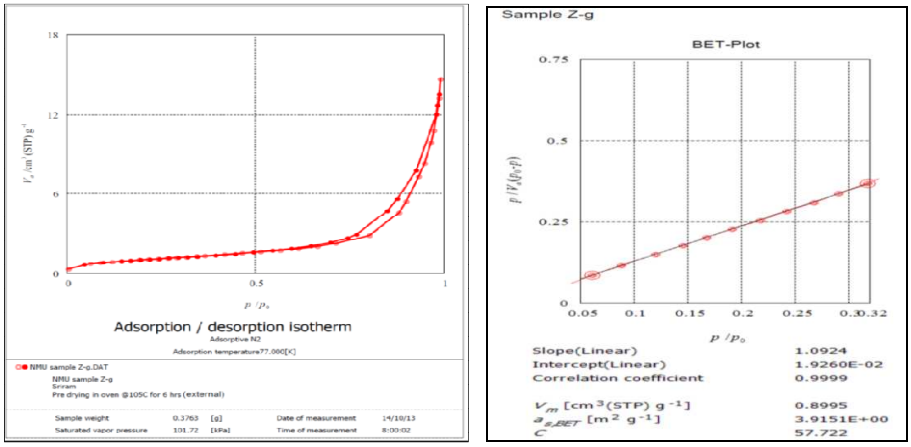

Fig. 6 & 7 BET N_2 Absorption/Desorption Isotherm & BET Particle Size Distribution Graph

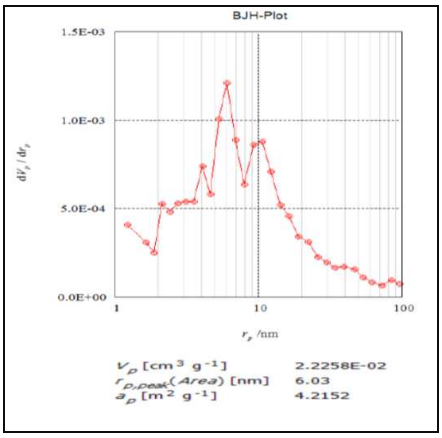

Fig. 8 BET Pore Size Distribution Graph

TGA Analysis

The thermo gravimetric analysis (Fig. 9) shows no degradation in original fly ash sample up to 800°C while the MFA shows two step degradation points. The first degradation occurs between 50–100°C due to absorbance of moisture from surrounding humid atmosphere. The second stage degradation occurs between 180 – 300°C due to breaking of highly acidic Fe-O bond resulting the formation of iron oxide and silica while the crystalline product decomposes to amorphous powders which is then stable up to 800°C. During the second degradation 20% weight loss is observed.

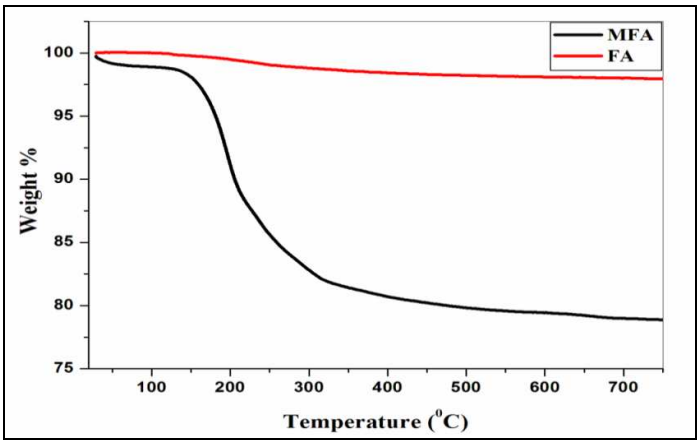

Fig. 9 Thermal Gravimetric Analysis.

XPS Analysis

The X-ray photo-electronic spectroscopic analysis of MFA depicts the presence of vanadium and cerium metal impurities along with iron, aluminium, silicon, oxygen and carbon as desired to present. The iron which is incorporated shows the binding energy of its valence electron at 716 eV which is far more than its binding energies in its oxides forms like FeO 709.8 eV and Fe_2O_3 comes at 710.8 which ultimately evident for its tetrahedrally binding with silicon through oxygen bridges. Same can be explained in case of silicon which also shows higher binding energy than its natural oxide SiO_2.

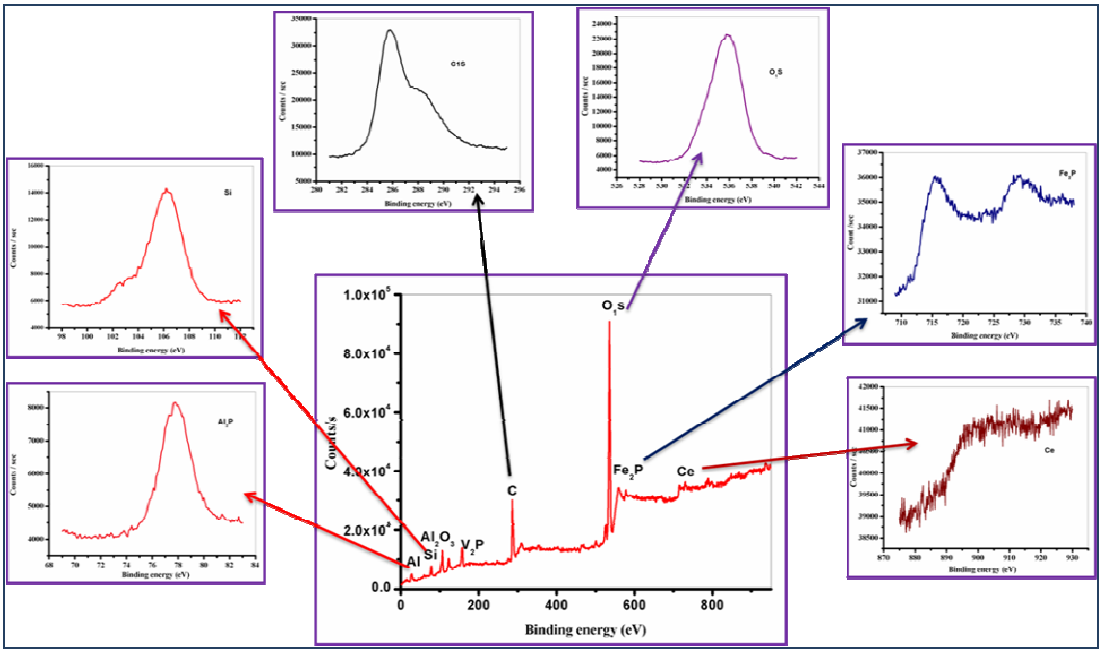

Fig. 10 X-Ray Photo-electronic Spectroscopic Analysis.

Table 1. List of Synthesized Azomethine Derivatives of INH

Sr. No.	Code	Ar	H/R	Product	Time (min)	Yield (%)	Melting Point (^{o}C)	Reported Melting Point (^{o}C)
1	**3a**	C_6H_5-	H	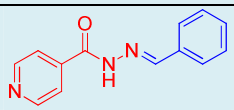	5	89	204-206	205-208[19]
2	**3b**	p-OH-C_6H_5-	H	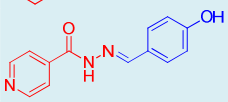	5	92	190-192	189-191[19]
3	**3c**	o-OH-C_6H_5-	H	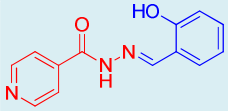	7	93	202-204	203-205[19]
4	**3d**	m-OH-C_6H_5-	H	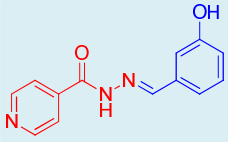	10	88	>250	--
5	**3e**	o-NO_2-C_6H_5-	H	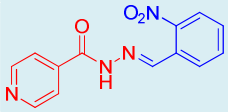	3	92	226-228	--
6	**3f**	m-NO_2-C_6H_5-	H	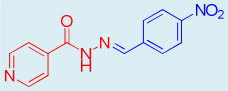	6	90	240-242	240-242[20]
7	**3g**	$C_{14}H_9$-	H	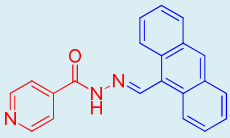	15	85	>250	--
8	**3h**	o-OCH_3-m-OCH_3-C_6H_4	H	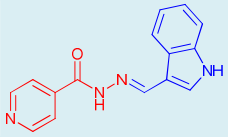	15	84	142-144	--

Note: The table contains the list of synthesized azomethine derivatives of INH with the required time for the synthesis, their yields and melting points.

The time required for reaction and yield of products after replacing the aldehyde derivatives are summarized in Table 1. The results depicts the EDGs at 2 and 4 positions enhances the rate of reaction with respect to time while in case of bulky substituent, there is retardation in the rate of reaction which can be attributed to the steric hindrance.

Table 2. Comparison Study of Catalysts.

Sr. No.	Catalyst	Time	Temperature (^{o}C)	Yield (%)
1	No Catalyst[20]	2-2.5 hour	Refluxed in EtOH	82%
2	Acetic acid[18]	3-4 hour	Refluxed in EtOH	82%
3	Fly Ash	2-3 hour	Refluxed in EtOH	85%
4	MFA	10-30 min	RT	89%

Note: The table for comparison of catalytic activity of MFA with parent fly ash and other reported catalysts.

The synthesized MFA is proved to be as energy efficient catalyst for the synthesis of azomethine derivatives of INH as it acts as heterogeneous catalyst reducing reaction time as

mentioned in earlier reports. The MFA comprises the porous crystalline nature having ferrous silicate constituent in which the iron and silicon are connected with oxygen bridges just like a zeolite. The replacement of homogeneous acid catalyst by solid acid catalyst is the main achievement of the present study as summarised in Table 2.

Characterizations of Synthesized derivatives

3a: (E)-N'-benzylidene isonicotinohydrazide, Melting Point = 204-206^{o}C, m/z =, Mass Analysis, base peak = M+1, H^1 NMR (DMSO, 400 MHz), δ_H = 1H (S 12.09), 2H (dd 8.76, 5.6 Hz, 16 Hz, 4 Hz) 1H (S 8.47), 2H (dd 7.83, 2.4 Hz, 2.8 Hz, 1.6 Hz) 2H (dd 7.75, 2.8 Hz, 5.2 Hz, 1.6 Hz) 3H (m 7.49, 0.4 Hz, 3.2 Hz, 5.2 Hz, 4.4 Hz, 2 Hz, 3.2 Hz, 1.6 Hz), C^{13} NMR (DMSO, 100 MHz) δ_C = 162.09, 150.81, 149.49, 140.93, 134.48, 130.87, 129.37, 127.74, 122.

3b: (*E*)-*N'*-(4-hydroxybenzylidene) isonicotinohydrazide, Melting Point = 190-192^{o}C, m/z = Mass Analysis, base peak = M+1, H^1 NMR (DMSO, 400 MHz), δ_H = 1H (S 11.80), 1H (S 9.88), 2H (Broad S 8.76), 1H (S 8.37), 2H (d 7.83, 3.68 Hz), 2H (d 8.22), 2H (d 7.85, 8.56 Hz), 2H (dd 6.80, 8.52 Hz, 8.36 Hz, 17.84 Hz), C^{13} NMR (DMSO, 100 MHz) δ_C = 161.25, 159.68, 150.04, 149.36, 140.55, 128.94, 128.44, 124.85, 121.40, 115.59.

3c: (*E*)-*N'*-(2-hydroxybenzylidene) isonicotinohydrazide, Melting Point = 202-204^{o}C, m/z = Mass Analysis, base peak = M+1, H^1 NMR (DMSO, 400 MHz), δ_H = 1H (S 12.29), 1H (S 11.17), 2H (dd 8.75, 5.64 Hz, 4.68 Hz, 18.12 Hz), 1H (S 8.67), 2H (d 7.85, 4.6 Hz, 1.32 Hz), 1H (m 7.54, 1.2 Hz, 1.2 Hz, 6.44 Hz), 1H (m 7.29, 7 Hz, 7.04 Hz, 1.48 Hz), 2H (dd 6.92, 8 Hz, 7.44 Hz, 7.12 Hz), C^{13} NMR (DMSO, 100 MHz) δ_C = 161.16, 157.62, 150.17, 149.47, 139.79, 131.46, 129.58, 121.37, 119.15, 118.32, 116.37.

3d: (*E*)-*N'*-(3-hydroxybenzylidene) isonicotinohydrazide, Melting Point = more than 250^{o}C, m/z = Mass Analysis, base peak = M+1, HRMS Analysis, $C_{13}H_{12}O_2N_3$ = 242.0924, Base peak = 242.0928, H^1 NMR (DMSO, 400 MHz), δ_H = 1H (S 11.99), 1H (S 9.57), 2H (d 8.76, 4.2 Hz), 1H (S 8.39), 2H (d 7.23, 3.2 Hz, 8.2 Hz), 1H (d 7.12, 7.6 Hz), 1H (d 6.86, 1.64 Hz), 1H (d 6.84, 1.72 Hz), C^{13} NMR (DMSO, 100 MHz) δ_C = 162.04, 158.17, 150.8, 149.57, 140.95, 135.74, 130.43, 121.99, 119.49, 118.23, 113.18.

3e: (*E*)-*N'*-(2-nitrobenzylidene) isonicotinohydrazide, Melting Point = 226-228^{o}C, m/z = 270, Mass Analysis, base peak = M+1, $C_{13}H_{11}O_3N_4$ = 271.0826, Base peak = 271.0832, H^1 NMR (DMSO, 400 MHz), δ_H = 1H (S 12.39), 1H (S 8.95), 2H (d 8.78, 5.76 Hz), 1H (t 8.19, 3.76 Hz, 4.12 Hz), 1H (d, 8.08, 8 Hz), 2H (d 7.86, 5.84 Hz), 2H (d 7.80, 7.56 Hz, 7.64 Hz), 1H (d 7.69, 6.24 Hz), 1H (7.65, 0.92 Hz), C^{13} NMR (DMSO, 100 MHz) δ_C = 161.76, 150.12, 148.17, 144.16, 139.9, 133.49, 130.64, 128.08, 124.48, 121.42.

3f: (*E*)-*N'*-(4-nitrobenzylidene) isonicotinohydrazide, Melting Point = 240-242^{o}C, m/z = 270, Mass Analysis, base peak = M+1, H^1 NMR (DMSO, 400 MHz), δ_H = 1H (S 12.36), 2H (Broad S 8.81), 1H (S 8.59), 1H (d 8.3), 1H (d 8.22), 2H (d 8.03), 2H (d 7.86).

3g: (*E*)-*N'*-(anthracene-9-ylmethylene) isonicotinohydrazide, Melting Point = more than 250^{o}C, m/z = 325, Mass Analysis, base peak = M+1, HRMS Analysis, $C_{21}H_{16}ON_3$ =

326.1288, Base peak = 326.1295, H^1 NMR (DMSO, 400 MHz), δ_H = 1H (S 12.28), 1H (S 9.70), 2H (d 8.32, 5.6 Hz), 2H (d 8.74, 8.84 Hz), 1H (S 8.65), 2H (t 8.13, 9.64 Hz, 8.28 Hz), 2H (d 7.95, 5.88 Hz), 2H (t 7.62, 6.84 Hz, 7.6 Hz), 2H (t 7.55, 7.6 Hz, 7 Hz), C13 NMR (DMSO, 100 MHz) δ_C = 161.47, 150.15, 148.15, 140.36, 130.84, 129.73, 128.81, 126.93, 125.27, 124.83, 124.74, 121.39.

3h: (E)-N'-((1H-indole-3-yl) methylene) isonicotinohydrazide, Melting Point = 142-144^{o}C, m/z =264, Mass Analysis, base peak = M+Na, M+1(87%), HRMS Analysis, $C_{15}H_{13}ON_4$ = 265.1084, Base peak = 265.1089, H^1 NMR (DMSO, 400 MHz), δ_H = 1H (S 11.78), 1H (S 11.67), 2H (d 8.79, 4.4 Hz), 1H (S 8.65), 1H (d 8.30, 7.56 Hz, 7.12 Hz), 3H (dd 7.87, 4.76 Hz, 10.64 Hz), 1H (d 7.47, 7.76 Hz) 2H (m 7.19, 6.88 Hz, 7.76 Hz, 5.32 Hz, 7.56 Hz, 7.08 Hz, 7.68 Hz.

Conclusion

In the present work, the modification of fly ash by incorporation of iron in its pozzolanic framework on calcination proved a key step for development of new heterogeneous catalyst (MFA). The synthesized MFA is confirmed as a very efficient catalyst as it has an ability to access the reactants to react in its pore voids. The MFA, by virtue of its acid sites polarizes the isonicotinohydrazide thereby reduces the Ea and the reaction occurs at RT with less time compared to the conventional methods. The synthesis of azomethine derivatives of INH utilizes green chemical pathway with less reaction time, energy efficiency, ease of separation and replacement of harmful acids by heterogeneous solid acid catalyst.

Acknowledgement

We are thankful to UGC, New Delhi for financial support through UGC R&D Project. We thank SAIF, Chandigarh, Punjab University for spectral data. We acknowledge support of Mr. Sachin Avhad, Territory Manager, Metrohelm India Limited, Navi Mumbai – 400 710 (MS) India for BET surface area and porosity analysis and characterization and CIF, UICT, NMU, Jalgaon for helping in terms of physical characterizations.

References:

1. a) V. Escande, A. Velati, C. Garel, B-L. Renard, E. Petit, and C. Grison, *Green Chem.*, 2015. b) I. Zohar, R. Bookman, N. Levin, H. de Stigter and N. Teutsch, *Environmental Science and Technology*, 2014, **48**, 13592-13600. c) R. C. Cioc, E. Ruijter and R. V. A. Orru, *Green Chem.*, 2014, **16**, 2958–2975.
2. a) O. Cheung and N. Hedin, *RSC Adv.*, 2014, **4**, 14480-14494. b) R. Chal, C. Gerardin, M. Bulut and S. V. Donk, *ChemCatChem*, 2013, **3**, 67-81.
3. a) H. L. Ngo, Lipid Technology, 2014, **26**, 11-12. b) J. H. Clark, *Acc. Chem. Res.*, 2002, **35**, 791-797.
4. a) A. Takagaki, J. C. Jung and S. Hayashi, *RSC Adv.*, 2014, **4**, 43785-43791. b) L. Wang, S. Yamamoto, S. Malwadkar, S-I, Nagamatsu, T. Sasaki, K. Hayashizaki, M. Tada, and Y. Iwasawa, *ChemCatChem*, 2013, **5**, 2203 – 2206. c) D. Perra, N.

Drenchev, K. Chakarova, M. G. Cutrufello and K. Hadjiivanov, *RSC Adv.*, 2014, 4, 56183-56187.
5. R. Y. Brogaard, C-M. Wang and F. Studt, *ACS Catal.*, 2014, **4**, 4504-4509.
6. M. Malhotra, G. Sharma and A. Deep, *Acta Poloniae Pharmaceutica – Drug Research*, 2012, **69 (4)**, 637-644.
7. M. Hermanek, R. Zboril, I. Medrik, J. Pechousek, and C. Gregor, *J. AM. CHEM. SOC.*, 2007, **129**, 10929-10936.
8. X. Querol*, N. Moreno, J.C. Uman˜a, A. Alastuey, E. Herna´ndez, A. Lo´pez-Soler, F. Plana, *International Journal of Coal Geology*, 2002, **50**, 413 – 423.
9. Y-q. Jin, X-j. Ma, X-g. Jiang, H-m. Liu, X-d. Li, J-h. Yan and K-f. Cen, *Energy Fuels*, 2013, **27**, 394−400.
10. J. Jiang, J. Yu and A. Corma, *Angew. Chem.*, 2010, **49**, 3120-3145.
11. X. Querol, N. Moreno, A. Alastuey, R. Juan, J. M. Andres, A. Lopez-soler, C. Ayora, A. Medinaceli and A. Valero, *Geologica Acta*, 2007, **5 (1)**, 49-57.
12. K. Li, J. Valla, J. G-Martinez, *ChemCatChem*, 2014, **6**, 46-66.
13. M. Malhotra, V. Monga, S. Sharma, J. Jain, A. Samad, J. Stables, A. Deep, *Med. Chem. Res.*, 2012, **21**, 2145-2152.
14. R. R. Somani, A. G. Agrawal, P. P. Kalantri, P. S. Gavarkar and E. D. Clercq, *International Journal of Drug Design and Discovery*, 2011, **2 (1)**, 353-360.
15. a) A. P. G. Nikalje, M. Pathan, M. Ghodke and D. Rajani, *Der Pharmacia Sinica*, 2012, **3(4)**, 488-493. b) K. Tayade, S. K. Sahoo, B. Bondhopadhyay, V. K. Bhardwaj, N. Singh, A. Basu, R. Bendre and A. Kuwar, *Biosensors and Bioelectronics*, **61**, 429-433.
16. N. Georgieve, Z. Yaneva, G. Nikolova and S. Simova, *Advances in Bioscience and Biotechnology*, 2012, **3**, 1068-1075.
17. S. Niazi, C. Javali, M. Paramesh and S. Shivaraja, *Int J Pharmacy Pharm Sci.*, 2010, **2 (3)**, 108-112.
18. G. Nigade, P. Chavan and M. Deodhar, *Med. Chem. Res.*, 2012, **21**, 27-37.
19. M. malhotra, V. Monga, S. Sharma, J. Jain, A. Samad, J. Stables and A. Deep, *Med. Chem. Res.*, 2012, **21**, 2145-2152.
20. M. M. Heravi, V. Zadsirjan, K. Bakhtiari and F. F. Bamoharram, *Synthesis and Reactivity in Inorganic, Metal-Organic, and Nano-Metal Chemistry*, 2013, **43**, 259-263.

1x0mm (600 x 600 DPI)